

Optimizing Support Patch Geometries in Adhesively Bonded Single Lap Joints: A Finite Element Analysis Approach

Ahmet Çalık ✉
Burdur Mehmet Akif Ersoy University, Department of Mechanical Engineering, Turkey
✉ acalik@mehmetakif.edu.tr

Abstract *In recent years, the preference for adhesive bonding over traditional methods like bolted or riveted connections has garnered the attention of researchers. This study employs finite element analysis to optimize the geometry and placement of support patches in adhesively bonded single lap joints, significantly reducing stress concentrations and enhancing joint strength. Initially, a comprehensive finite element analysis was conducted to numerically evaluate the influence of different support patch parameters and their positions on the strength of single lap joints (SLJs). To validate the finite element analyses (FEA), comparisons were made with existing studies in the literature and analytical solutions. The numerical results in this study reveal that the dimensions and placement of the support patch can potentially reduce the load and stress distribution in different regions of the adhesive joint, which could increase its strength.*

Keywords *Adhesive bonding, stress optimization, support patch geometry, finite element analysis.*

Highlights

- *Identified optimal support patch geometries to reduce stress in SLJs, improving durability and load distribution.*
- *Findings provide insights for stronger adhesive joints in aerospace, automotive, railway, and construction.*
- *3D finite element analysis shows how patch thickness, position, and length affect stress and joint performance.*

1 INTRODUCTION

Adhesive bonding, renowned for its high mechanical performance, is a widely preferred assembly technique in industries like automotive, aerospace, electronics, and construction [1-3]. Despite the extensive use of adhesive bonding in aerospace and automotive industries, stress concentration remains a critical challenge in single lap joints (SLJs). This issue significantly limits the joint's load-carrying capacity and durability, especially under dynamic or cyclic loading conditions. Its popularity arises from its ability to create strong, reliable joints in demanding applications [4]. Adhesive bonded joints are particularly effective when subjected to shear forces. SLJs are commonly used in adhesive bonding due to their straightforward geometry and easy application [5, 6]. Moreover, SLJs serve as an effective method in achieving structural integration and often exhibit high mechanical performance. This type of joint facilitates load transfer by leveraging the adhesive's shear properties. Therefore, SLJs are a preferred choice for many industrial applications, especially in the automotive and aerospace sectors [7].

The finite element method (FEM) has been extensively utilized to forecast the performance of joined structures. FEM provides numerous benefits, such as the ability to alter boundary conditions, modify the geometry of the structure, and analyze structures constructed from diverse materials. It also permits the assessment of how alterations in various parameters affect the behavior of bonded joints through intricate studies involving three-dimensional modeling. These models, coupled with effective failure criteria, are employed to scrutinize the distribution of stress in bonded joints and to anticipate potential failures. Research on adhesive bonding has primarily concentrated on the adhesive layer, which is identified as the vulnerable point in the assembly due to its mechanical characteristics [8]. While previous studies focus on adhesive properties or joint geometry, the combined influence of support patch parameters on stress distribution and joint performance remains unexplored. This knowledge gap hinders the development of more robust and durable adhesive joint designs.

The SLJ is a frequently employed joint type in various industries because of its uncomplicated geometry. Nevertheless, when such joint is under tension, an eccentric load leads to a bending moment in its overlapping area. This generates peel stresses, which can lead to damage at the edges of the joint overlap region [9]. In adhesive-bonded joints, there are various approaches to reduce the significant stress concentration that affects the strength of the connection. On the other hand, the fundamental drawback of this joining technique is the persistent high-level stress concentration at the overlap edges, due to the slow transfer of loads in adhesively bonded joints and the rotation of adherends in the presence of asymmetric loads. There are various bonding combinations available, leading to different stress distributions and levels of strength. Nevertheless, the SLJ is the prevailing choice due to its straightforward manufacturing process. To avert premature failure of the SLJ, mitigating stress concentration along the adhesive edges is paramount. This paper addresses this gap by systematically analyzing the effects of support patch geometries on stress distribution using advanced 3-dimensional (3D) finite element (FE) modeling. The study evaluates how patch thickness, position, and length influence stress mitigation in SLJs, providing actionable insights for industrial applications. Assessing stress and strain distributions in these configurations is challenging due to the intricate geometry and varied material properties employed in this investigation. The generation of peel stresses at the visible edges of the overlap area is a pivotal factor influencing the mechanical robustness of adhesive connections. Mitigating these stresses, responsible for joint damage, enhances overall joint strength and, consequently, improves load-bearing capabilities. Various methods found in the literature have been employed to alleviate stresses at

 DOI: 10.5545/sv-jme.2025.1265

both extremities of the bonding zone [10-13]. The alterations in the shape of SLJs represent a frequently employed strategy to mitigate stress distribution issues in adhesively bonded joints, a concept widely explored in existing literature. Adhesive fillets, as part of these geometric modifications, offer a practical means to diminish stress concentrations specifically at the edges of the joint overlap [14-18]. This study provides a detailed analysis of the effects of support patch geometry on stress distribution within adhesively bonded SLJs. While previous research has focused primarily on the adhesive layer and overall joint geometry, this work specifically addresses the combined effects of various support patch parameters.

Amaro et al.'s [10] study systematically explored the impact of inside and outside tapers (30°, 45°, 60°) on adhesive joints using optical and electrical methods. Numerical analyses identified taper geometries leading to higher adhesive compression. Experimental and numerical results concurred that reducing taper angles enhances joint strength, with outside tapers exhibiting superior tensile/shear strength. Despite similar mid-line shear-peel loads, the inside taper, inducing more compression and non-coincident peak stresses, emerged as the preferred configuration. These findings offer crucial insights for optimizing adhesive joint design.

Durmus and Akpinar's [19] study delves into adhesive bonding, a common method of joining materials, focusing on the SLJ type. The research addresses issues such as peel stress and damage in adhesively bonded joints, proposing the step-lap joint as a solution. By experimentally and numerically examining SLJ, one-step lap joint (OSLJ), and three-step lap joint (TSLJ) under tensile loading, the study highlights TSLJ's superior load-bearing capacity. Results reveal the significant impact of step length variation in TSLJ on joint failure loads. Experimental and numerical findings, employing the cohesive zone model, demonstrate good agreement. The study also determines the optimal length for the initial step in the TSLJ overlap area.

Marques and da Silva [20] study addresses aircraft damage, proposing adhesive-bonded patches as a repair method. Traditional techniques using screws or rivets create stress concentrations, leading to undetectable new cracks. To improve long-term behavior and reduce costs, the aeronautical industry explores patches with a taper, spew fillet, and dual adhesives. Experimental testing on aluminum alloy sheets shows advantages for brittle adhesives with a taper and dual adhesive for taperless configurations.

The influence of cohesive law shapes on the behavior of adhesively bonded patch repairs has been a focus of research. Fernandez-Canadas et al. [5], investigated the cohesive failure of the adhesive layer in single-lap joints under uniaxial tensile loads. In this study, a three-dimensional FE model was developed using Abaqus, comparing the effects of different cohesive law shapes, including linear, exponential, and trapezoidal, on the failure load of the joints. Their findings indicated that the trapezoidal law provided the best fit to experimental data due to its ability to capture the plastic flow of the adhesive, highlighting the importance of selecting an appropriate cohesive law shape based on the adhesive's behavior.

Andruet et al. [21] developed 2D and 3D adhesive elements for stress analysis in bonded joints, incorporating geometric nonlinearity to account for large displacements. Their model effectively reduces computational requirements while providing accurate predictions, as demonstrated in SLJs and crack patch geometries. This highlights the importance of advanced modeling techniques in adhesive joint design.

Demiral and Mamedov [22] examined the fatigue performance of adhesively bonded step-lap joints under tensile loads, finding that increasing the number of steps improved the joint's fatigue resistance. Paygozar et al. [23]'s study focuses on predicting failure loads of adhesive double-strap joints through validated FE analyses. The dimensions of the patch significantly impact the failure load and stress distribution in various joint parts, potentially affecting joint performance. Results reveal similar performance between aluminum and composite straps, with the latter having an advantage when considering added weight to the system.

While the FEM has been extensively used to analyze the behavior and performance of adhesively bonded SLJs, this study introduces new insights into the optimization of support patch geometries. Unlike previous research, which has largely focused on the adhesive layer and overall joint geometry, the investigation specifically targets the nuanced effects of support patch parameters including thickness, position, length, and their combined influence on stress distribution and joint strength. This research analyzes a wide range of support patch configurations using a detailed parametric study. The novelty of the approach lies in the integration of multi-parameter variations to pinpoint the most influential factors contributing to the performance enhancement of adhesive bonded SLJs. The author employs advanced 3D FE analysis to capture the complex interplay between these variables, providing a more in-depth understanding of their impact on the mechanical behavior of the joint.

Furthermore, the study ventures beyond the typical analysis by comparing the numerical results with existing studies and analytical solutions like Volkersen [24] and Goland and Reissner [25], offering a validation perspective seldom taken in the literature. The resulting data set and findings are unique in their breadth and depth, delivering actionable insights for the design of more robust and efficient adhesive joints in industrial applications. By pushing the boundaries of current analytical methods and exploring the combined effects of various patch geometries, this study advances state-of-the-art in the FE analysis of adhesively bonded single lap joints (ABSLJs). The effect of the support patch on the outer part of the adherent layer of adhesively bonded SLJs on the stress distribution within the joint was investigated. A comprehensive FE analysis was conducted to numerically evaluate the influence of different support patch parameters and their positions on the strength of SLJs. The results showed that the dimensions and placement of the support patch have the potential to reduce the load and stress distribution in different regions of the adhesive joint, thereby potentially increasing its strength.

The findings contribute to closing the gap between theoretical research and practical, real-world applications, setting a precedent for future experimental validations and innovative design strategies in structural joint assemblies.

2 MATERIAL AND METHODS

The SLJ serves as a standard benchmark in adhesive comparisons, characterized by a non-uniform stress distribution along the adhesive thickness and lap length. Several factors intricately influence the shear and peel stresses within this joint assembly. The effectiveness of the joint is significantly impacted by adhesive application methods, surface preparation, physico-chemical properties of the adhesive, assembly dimensions, and adhesive thickness. The adhesively SLJ, renowned for its simplicity, finds extensive use with adherents composed of metallic or fiber composite materials. This joint type is a subject of frequent investigation to comprehend its strength and characteristics. Notably, the SLJ stands out for its uncomplicated design and ease of assembly, making it a cost-effective and widely employed configuration. In this study, adherence to the ASTM D1002 standard [25] for determining joint shear strength ensures consistency and reliability in the evaluation process.

2.1 SLJ Dimensions

The SLJ dimensions include a 0.18 mm adhesive thickness (t), 2 mm adherent thickness (k), 25 mm lap length, and 25 mm substrate width (w). The parametrically studied parameters, thickness of the support patch (u), the adhesive thickness bonding the support patch to the adherent (s), length of the support patch (d), and position of the support patch (e) are presented in Table 1. The position of the support piece, denoted as the distance between the adherent end (q) and the midpoint of the support piece, is shown in Figs. 1 and 2. The directions are indicated as longitudinal (x) and transverse (y), while the z–axis aligns with the substrate width direction.

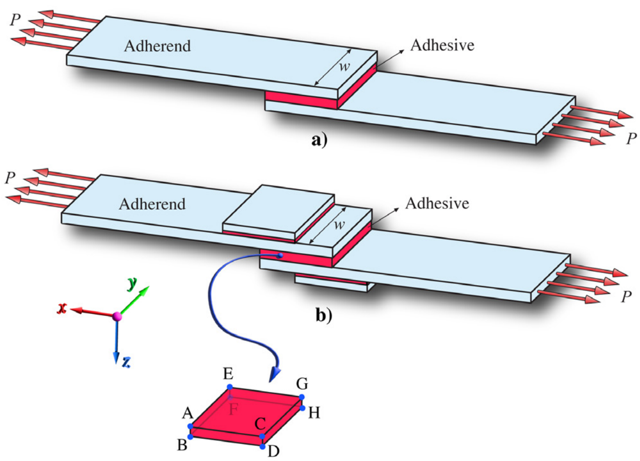

Fig. 1. 3D Support-patched SLJs

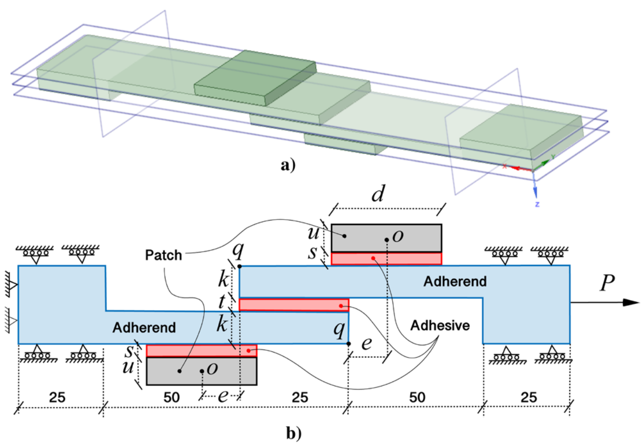

Fig. 2. Support-patched SLJs; a) ANSYS model, and b) geometry and boundary conditions

2.2 FE Analysis Setup and Loading Conditions for SLJ

In the FE analysis, the upper substrate of the adhesive joint was fixed at one end in a single bottom configuration, while the overlapping substrate was subjected to an axial force (F) at the opposite end. The transverse movement of the overlapping substrate was constrained, as indicated in Fig. 1. The end where the loading occurred retained the freedom to move along the x axis. Subsequent loading was applied to validate and predict the structural response for this specific analysis. Fig. 2 provides a visual representation of the loading conditions and constraints (boundary conditions, BC) essential for the analysis of the SLJ. This configuration allows for a comprehensive examination of the joint's behavior under applied loads, facilitating a thorough understanding of its structural performance.

In the FE analysis of the SLJs, careful consideration was given to the mesh configuration to optimize accuracy and computational efficiency. The model primarily utilized hexahedral mesh elements due to their suitability for capturing the complex stress gradients typical in adhesive joints. A convergence study was performed to determine the appropriate mesh density, particularly focusing on areas of high stress concentration where finer meshing was necessary. The advanced 3D FE analysis captures the complex interactions of support patch geometries. This methodology goes beyond existing 2D models, providing a more realistic simulation of the three-dimensional stress distribution in adhesive joints.

Table 1. The configuration of the SSLJ

Sp.	u [mm]	s [mm]	e [mm]	d [mm]	Joint type
1	-	-	-	-	SLJ
2	k	t	0	l	SSLJ
3	$k/2$	t	0	l	SSLJ-K2
4	$k/4$	t	0	l	SSLJ-K4
5	k	$t/2$	0	l	SSLJ-T2
6	k	$t/4$	0	l	SSLJ-T4
7	k	t	0	$l/2$	SSLJ-L2
8	k	t	$d/4$	$l/2$	SSLJ-D4-L2
9	k	t	$d/2$	$l/2$	SSLJ-D2-L2
10	k	t	$d/4$	l	SSLJ-D4
11	k	t	$d/2$	l	SSLJ-D2
12	k	t	0	$3l/2$	SSLJ-3L2
13	k	t	$d/4$	$3l/2$	SSLJ-D4-3L2
14	k	t	$d/2$	$3l/2$	SSLJ-D2-3L2
15	k	t	0	$2l$	SSLJ-2L
16	k	t	$d/4$	$2l$	SSLJ-D4-2L
17	k	t	$d/2$	$2l$	SSLJ-D2-2L

Surface interactions between the adhesive layer and the adherends were modeled using cohesive zone models (CZM) to simulate the potential delamination and failure modes realistically. This approach allows for the consideration of both the mechanical properties of the materials and the interface behavior under load. Tie constraints were applied where necessary to ensure that the movement between the adherends and the adhesive was realistically constrained, reflecting the physical bond. These constraints were essential in modeling the load transfer across the joint without slippage, which is critical for assessing the joint's integrity under stress.

2.3 Material Properties of Adhesive and Adherend

In this study, DP-460NS was utilized as the adhesive, with Aluminum 6061 serving as the adherend material in SLJs. DP-460NS is an epoxy adhesive manufactured by the company 3M, known for its chemical resistance and environmental durability [21]. It requires a mixing ratio of 2 parts resin to 1 part hardener, with a working time of approximately 20 to 30 minutes and full cure of about 24 hours at room temperature. It is suitable for bonding a variety of materials and is commonly used in aerospace, automotive, electronics, and general industrial applications. Aluminum 6061 is a popular alloy known for its excellent combination of strength, weldability, and corrosion resistance. It falls within the category of 6000 series aluminum alloys, a class distinguished by its predominant composition of aluminum, accompanied by the alloying elements magnesium and silicon [27]. The alloy's composition, characteristic of the broader series, imparts it with unique properties and versatile applications across various industries [23]. The material properties of the adherent and adhesive are presented in Table 2.

Table 2. Material Properties [28]

Material	Young's modulus [GPa]	Poisson ratio	Yield stress [MPa]	Tangent modulus [GPa]
Aluminum 6061	71	0.33	125	1.48
DP460-NS Adhesive	2.2	0.41	36	0.5

In this study, the adhesive layer was modeled using the CZM. CZM operates by utilizing the relationship between stresses and relative displacements and exhibits elastic behavior up to the cohesive strength (in tension, T_n; in shear, T_t) [28]. For analysis with CZM, it is essential to know the parameters $\sigma_{n\max}$, G_{IC}, $\tau_{t\max}$, and G_{IIC}, where $\sigma_{n\max}$ is is the maximum normal cohesive strength (32.6 MPa), G_{IC} is the mode I fracture energy (2.56 N/mm), $\tau_{t\max}$ is the maximum shear cohesive strength (28.5 MPa), and G_{IIC} is the mode II fracture energy (11.71 N/mm). The CZM parameters used in the analysis are provided in Table 3.

Table 3. CZM parameters of the adhesive [29]

Parameter	Value	Parameter	Value
$\sigma_{n\max}$ [MPa]	32.6	$\tau_{t\max}$ [MPa]	28.5
G_{IC} [N/mm]	2.56	G_{IIC} [N/mm]	11.71

2.4 Support Patch Geometry

Adhesive-bonded joint with support patch was analyzed using FEA with 21 different parameters to investigate its effect on the peel and shear stress distributions on the bonded joint adhesive surface. In order to compare the results, a classical SLJ analysis was also performed. To examine the influence of support patch thickness on the joint strength, three different values were considered. Additionally, three values of adhesive thickness (s) connecting the support patch were investigated. Furthermore, a 12-parameter analysis was conducted to study the effects of support patch length (d) and position (e). The results are presented below.

2.5 FE analysis of SLJ

Boundary conditions are critical for the accuracy of FE simulations. In this study, the boundary conditions were designed to replicate realistic service conditions of the SLJs. The ends of the adherends were constrained to mimic the fixed and free ends typically encountered in engineering applications, allowing for a detailed analysis of stress distributions under applied loads.

The model utilized hexahedral volume elements for their balance of accuracy in capturing stress gradients and efficiency in computation. Hexahedral elements, particularly well-suited for modeling regular geometries, provided a structured mesh conducive to capturing the mechanical behavior of the adhesive joint.

Mesh density is a pivotal factor in FE analysis, with a finer mesh typically leading to more accurate results. An iterative mesh refinement procedure was conducted to ascertain the optimal mesh density. Starting with a coarse mesh, the number of elements was progressively increased until the shear stress values at specific points of interest on the adhesive layer stabilized. This approach ensured that the mesh was sufficiently refined in the overlap and other regions of discontinuity, where stress gradients are the steepest, without unnecessarily increasing the computational load.

Fig. 3 depicts the meshing strategy utilized in the FE model. It highlights the refined mesh in the overlap area, reflecting the higher density of elements where the most significant stress variations are expected. The final mesh consisted of 662582 hexahedral elements and 2872700 nodes, providing the resolution required to accurately capture the essential stress characteristics of the SLJs.

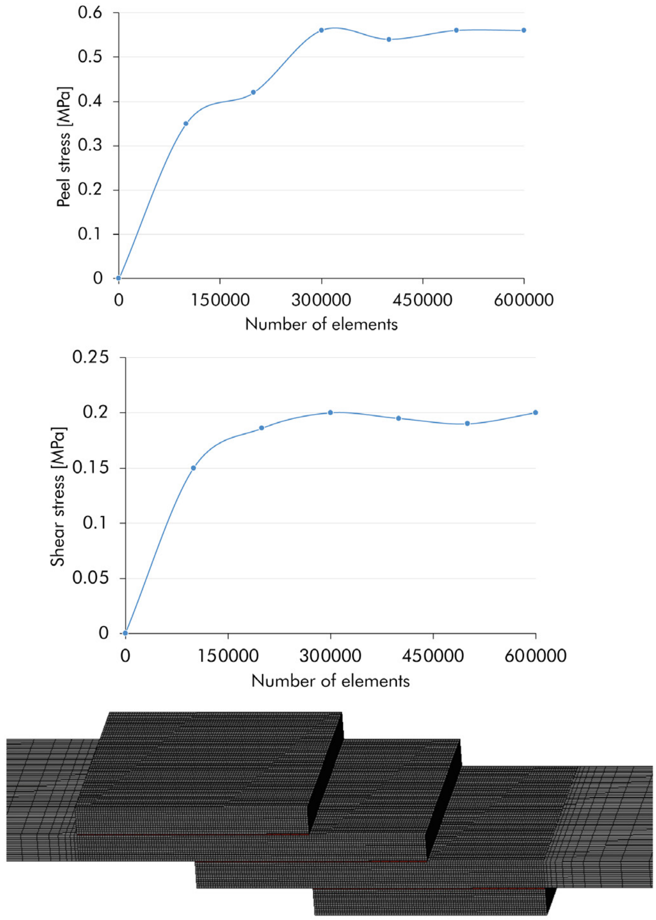

Fig. 3. FE mesh converge and the FE model of SLJ

2.6 Analytical Solutions

The Volkersen solution, which neglects the bending moment, is an analytical model used to analyze the adhesive shear stress distribution in a SLJ (Fig. 4). This model was developed by Volkersen in 1938 [24]. Also known as the "shear-lag model," it takes into account the differential shear of the adhesive in different regions. It is used to estimate the varying adhesive shear stress distribution along the bond line as in [30, 31].

When the substrates are of the same thickness, the shear stress reaches its maximum value. Therefore, it will be considered that the substrates have the same thickness. Furthermore, if the lap joint region also has equal length (l) and width (w), the equation simplifies as follows [31, 32]

$$\tau(x) = \sigma_{xz} = \frac{P\Psi}{2l^2}\left[\frac{\cosh[\Psi x]}{\sinh\left(\frac{\Psi L}{2}\right)}\right], \tag{1}$$

where

$$\Psi = \sqrt{\frac{2G_a}{Ekt}}. \tag{2}$$

Eq. (1) is applicable under the condition that the thicknesses of the two adherends are equal.

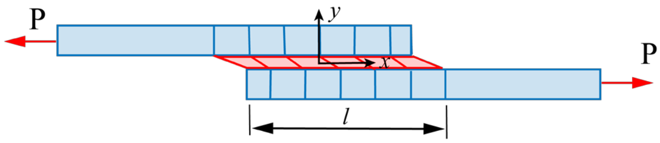

Fig. 4. Volkersen scheme for SLJ

The Goland and Reissner [25] analysis, which represents another analytical approach, is employed to assess the stress distribution in SLJs. This analysis assumes that the adhesive is elastic and that the adhesive layers are significantly stiffer. It takes into account the effects of rotation of the adherends, as shown in Fig. 5. Furthermore, the analysis considers the shear deformation of the adhesive layers [32]. The analysis provides equations that describe the adhesive shear stress distribution along the joint.

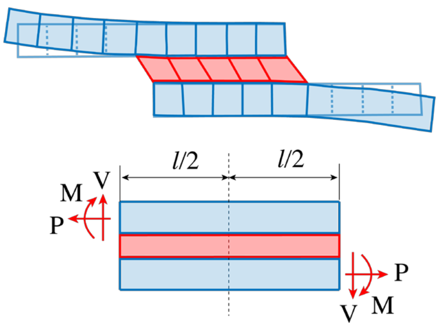

Fig. 5. Goland and Reissner scheme of SLJ

The formula for the distribution of adhesive shear stress τ according to Goland and Reissner [25] is given by the expression:

$$\tau = -\frac{1}{4}\frac{P}{l}\left\{\frac{\beta l}{2k}(1+3b)\frac{\cosh\left(\frac{\beta l}{2k}\frac{2x}{l}\right)}{\sinh\left(\frac{\beta l}{2k}\right)} + 3(1-b)\right\}. \tag{3}$$

Parameter b corresponds to the bending moment factor, which is derived from [25] and cited in [32].

$$b = \frac{\cosh\left(u_2\frac{l}{2}\right)}{\cosh\left(u_2\frac{l}{2}\right) + 2\sqrt{2}\sinh\left(u_2\frac{l}{2}\right)}, \tag{4}$$

where $u_2 = \sqrt{\frac{3(1-\nu^2)}{2}}\frac{1}{k}\sqrt{\frac{P}{kE}}$ and $\beta^2 = 8\frac{G_a E}{kt}$ is Poisson's ratio.

In the equations presented in this section, the variables are the following; E, elastic modulus [MPa], t, adhesive thickness [mm], k adherend thickness [mm], G_a shear modulus of adhesive [MPa], σ normal stress [MPa], τ, shear stress [MPa], P applied load [N], l overlap length [mm], Ψ parameter related to shear stress distribution [-], and b bending moment factor [-].

3 RESULTS AND DISCUSSIONS

3.1 Validation of the Current Numerical Study

Fig. 6 presents the adhesive shear stresses comparing the results from the current study with those from a numerical study by [7] and two analytical solutions [24, 25]. It validates the results of the study by using a SLJ with identical geometry and boundary conditions (support and loading) as those used in the referenced studies.

The comparison highlights significant differences between the 2D analytical solutions and the 3D FE analysis. The 2D models, while offering insights into shear and peel stress distributions, simplify the stress state by ignoring out-of-plane effects that are crucial for certain joint configurations. The 3D FE analysis incorporates these out-of-plane stresses, providing a more comprehensive understanding of the stress distributions across the adhesive joint. Notably, both shear and peel stresses were observed to be symmetric around the center of the joint length, reaching values significantly higher than those predicted by Volkersen 2D model. This discrepancy is mainly due to the 2D model's inability to effectively simulate the complex 3D stress state, particularly under multi-axial stress conditions.

Additionally, the Goland & Reissner model, although also 2D, includes considerations for the rotational stiffness of the adherends, offering a closer approximation to real-world conditions under certain loadings. This model displayed increased stress under specific conditions, likely influenced by moment effects not accounted for in simpler 2D models.

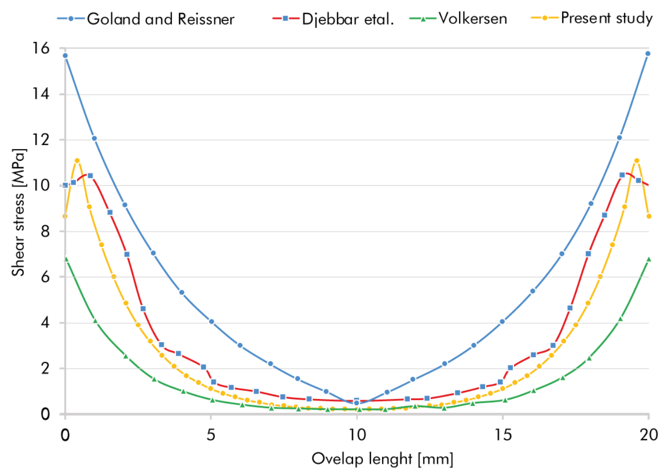

Fig. 6. Shear stress distribution from the finite element analysis of a SLJ, compared with analytical solutions

In conclusion, this comparative analysis emphasizes the critical role of 3D modeling for a more accurate representation of stress distributions in adhesive joints, especially in configurations where out-of-plane stresses are significant. However, 2D models still hold value for preliminary analyses in scenarios with minimal out-of-plane effects, due to their computational efficiency and simpler analytical approach. The choice between using 3D and 2D modeling should be guided by the specific requirements of the joint configuration. The results confirm that both the analytical and FE models provide coherent data that accurately predict joint behavior in SLJs, affirming the validity and reliability of the FE analysis.

3.2 Numerical Results

This section aims to investigate the effects of adhesive thickness, position, length, and thickness of reinforcement patches on the stress distributions of various SSLJs. To achieve this goal, a series of SLJs were simulated using the FE model in ANSYS software [33], incorporating various reinforcement patch configurations. These simulations encompass a range of SLJs with different parameter combinations, as detailed in Table 1. The obtained numerical results were analyzed to determine the optimized effects of varying adhesive thicknesses, positions, lengths, and thicknesses on the stress distributions of SLJs, aiming to identify the most suitable configuration.

Fig. 7 presents the peel stress distribution on the surface of a representative adhesive region. This distribution corresponds to the BDHF surface area depicted in Fig. 1. To facilitate a comparison of parametric analysis results, the stress distributions considered are along the 'overlap length' referred to as the BD line with the bonding region shown in Fig. 1. All two-dimensional graphs in this study are derived from stress distribution analyses along this BD line.

When adhesively bonded SLJs are subjected to bending loads, it is observed that the plates near the bonding area tend to bend outward. This bending notably increases the peel stresses within the adhesive region. In this study, the addition of a support patch to the bonded plate aims to reduce bending and, consequently, decrease peel stresses. The effects of the geometric dimensions and positioning of the support patch on the stress distribution will be thoroughly investigated.

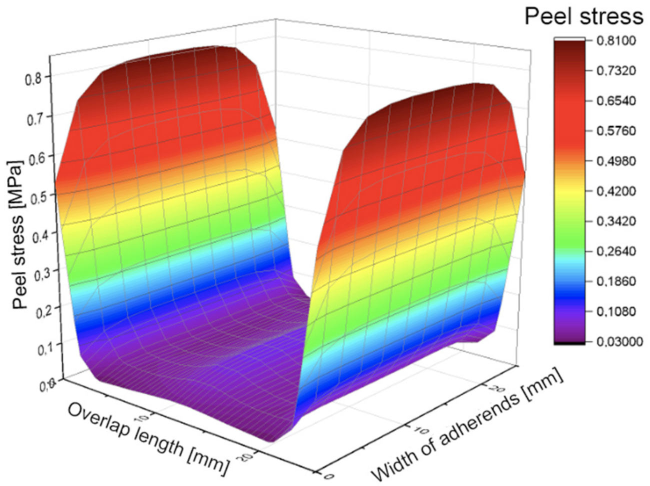

Fig. 7. 3D Stress distribution on the surface of the overlap region

3.3 Effect of Support Patch Thickness

To examine the influence of support patch thickness on the adhesive region, FE analysis was conducted for three different support patch thicknesses. The adhesive thickness used in the analysis was selected to be equal to the thickness of the support patches (i.e., denoted as $s=t$ in Fig. 2). Additionally, in the analysis, the center point (O) of the support patch and the points at the ends of the bonded plate (q) were aligned in the same vertical direction (i.e., set as $e=0$ in Fig. 2). Moreover, the patch length was chosen to be equal to the bonding length in the analysis (i.e., set as $d=l$ in Fig. 2).

For the purpose of comparing analysis results, changes in peel stress along the bonding length are presented graphically in Fig. 8a, while the shear stress results are illustrated in Fig. 9a.

Upon examination of Fig. 8a, it is observed that, at the edges of the adhesive region, there is a peel stress reduction of up to 70 % when compared to a SLJ with the same boundary conditions. This indicates significant alterations in the adhesive region.

In SSLJs, as the support patch thickness increases, peel stress values in the central regions of the adhesive area vary compared to SLJ. A decrease of 12 % for $u=k/4$, 25 % for $u=k/2$, and 40 % for $u=k$ is observed. However, an increase in support patch thickness has not caused a significant change in stress values at the edges.

Examining Fig. 9a, it can be seen how shear stress values change in the central regions of the adhesive area as the support patch thickness increases. A reduction of 11 % for $u=k/4$, 18 % for $u=k/2$, and 29 % for $u=k$ is recorded compared to SLJ. Peel and shear stress values in the middle sections of the bonded overlap region decrease proportionally with an increase in support patch thickness. Additionally, the increase in support patch thickness has led to a more pronounced decrease in peel stress than observed for shear stress.

3.4 Effect of Support Patch Adhesive Thickness

To investigate the influence of adhesive thickness specific to the support patch on the bonding region of the main plates, FE analysis was conducted for three different adhesive thicknesses of the support patch. In the analysis, the thickness of the main plates bonded with adhesive and the thickness of the support patches were chosen to be equal (i.e., denoted as $u=k$ in Fig. 2). Additionally, in the analysis, the center point (O) of the support patch and the points at the ends of the bonded plate (q) were aligned in the same vertical direction (i.e., set as $e=0$ in Fig. 2). Moreover, the patch length was selected to be equal to the bonding length in the analysis (i.e., set as $d=l$ in Fig. 2).

For the purpose of comparing analysis results, changes in peel stress along the bonding length are presented graphically in Fig. 8b, while the shear stress results are illustrated in Fig. 9b.

In SSLJs, selecting the same thickness for the adhesive bonding the support patch (s) and the adhesive bonding the main plates (t) reduces peel stress at the edges of the bonding region by 71 % compared to SLJ. Choosing the patch adhesive thickness as half of t ($s=t/2$) or one-fourth of t ($s=t/4$) yields the same peel and shear stress results along the bonding length. Additionally, selecting the patch adhesive thickness equal to t reduces the maximum value of peel stress by 64 % compared to when s is half of t ($s=t/2$) or one-fourth of t ($s=t/4$), without causing any change in shear stress values. Selecting specific ratios for patch adhesive thicknesses in SSLJs significantly reduces peel stress without affecting shear stress values. These findings can provide guidance in the optimal selection of adhesive thicknesses in structural joint design.

3.5 Effect of Support Patch Position

To investigate the influence of support patch length (d) when the bonding length is two times smaller ($l=d/2$), analyses were conducted for different patch positions (e) of 0, $d/4$, and $d/2$. The results revealed that the lowest peel stress at the edges and center of the bonding region occurred at $e=0$, as observed in Figs. 8c and 9c. The peel stress value at the edges of the bonding region at $e=0$ is 68 % lower than at $e=d/4$ and 74 % lower than at $e=d/2$. It was also determined that the shear stress values were the same at all three positions.

For cases where the support patch length is equal to the bonding length ($d=l$), results for patch positions of 0, $d/4$, and $d/2$ showed that the lowest peel and shear stress values at the edges and center of the bonding region occurred at $e=0$, as observed in Figs. 8d and 9d. The peel stress value at the edges of the bonding region at $e=0$ is 63 % lower than at $e=d/4$ and 75 % lower than at $e=d/2$. Additionally, the shear stress value at the edges of the bonding region at $e=0$ is 60 % lower than at $e=d/4$ and $e=d/2$.

When the support patch length is 3/2 times the bonding length ($d=3l/2$), results for patch positions of 0, $d/4$, and $d/2$ showed that the highest peel stress at the edges of the bonding region occurred at $e=d/4$, as observed in Fig. 8e. Peel stress values at the edges of the bonding region at $e=0$ and $e=d/2$ positions are the same and 2 % lower than at $e=d/4$. Peel stress at the center of the bonding region at $e=0$ is 50 % lower than at $e=d/4$ and 40 % lower than at $e=d/2$, as observed in Fig. 8e. Additionally, shear stress values at the edges of the bonding region at $e=d/4$ and $e=d/2$ positions are the same and 12 % higher than at $e=0$. Shear stress values at the center of the bonding region at $e=0$ and $e=d/4$ positions are the same and 14 % higher than at $e=d/2$.

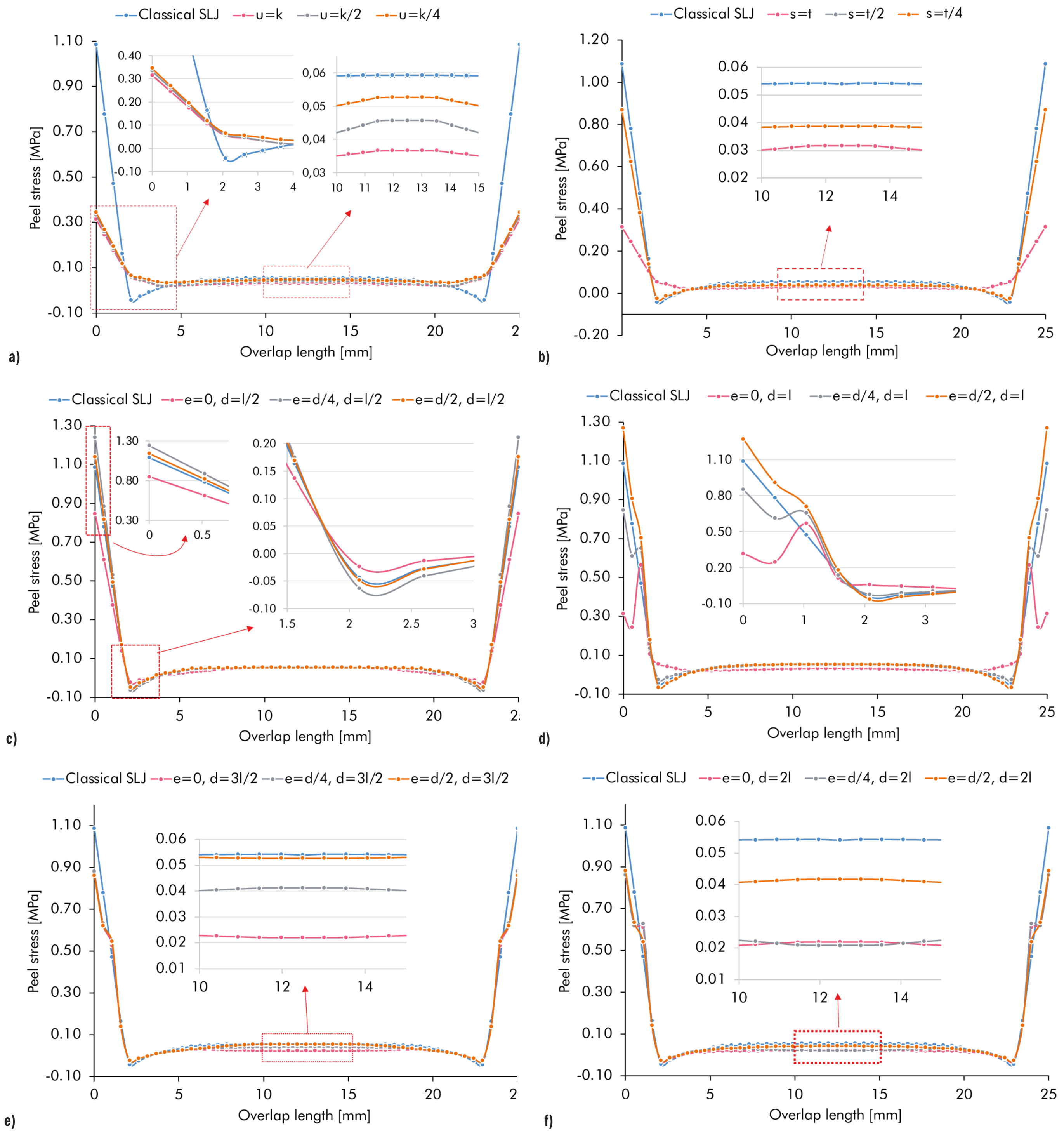

Fig. 8. Peel stress distribution along the length of the overlap zone

When the support patch length is twice the bonding length ($d=2l$), analyses for patch positions of 0, $d/4$, and $d/2$ showed that the highest peel stress at the edges and center of the bonding region occurred at $e=d/2$, as observed in Fig. 8f. Peel stress values at the edges and center of the bonding region at $e=0$ and $e=d/4$ positions are the same and 2 % lower than at $e=d/2$. For those cases the lowest shear stress at the edges and center of the bonding region occurred at $e=0$, as observed in Figs. 9e and f. The shear stress value at the edges of the bonding region at $e=0$ is 16 % lower than at $e=d/4$ and 30 % lower than at $e=d/2$. The shear stress values at the center of the bonding region at $e=0$ is 7 % lower than at $e=d/4$ and 12 % lower than at $e=d/2$.

3.6 Effect of Support Patch Length

When the support patch is positioned at $e=0$, the author conducted analysis for different lengths of the support patch ($d=l/2$, l, $3l/2$, and $2l$). Notably, when the support patch length matches the adhesive length ($d=l$), the author observed the lowest peel stress at the edges of the bonded region (Figs. 8c, d, e, and f). In this scenario, the peel stress at the edges is 36 % lower compared to cases with $d=l/2$,

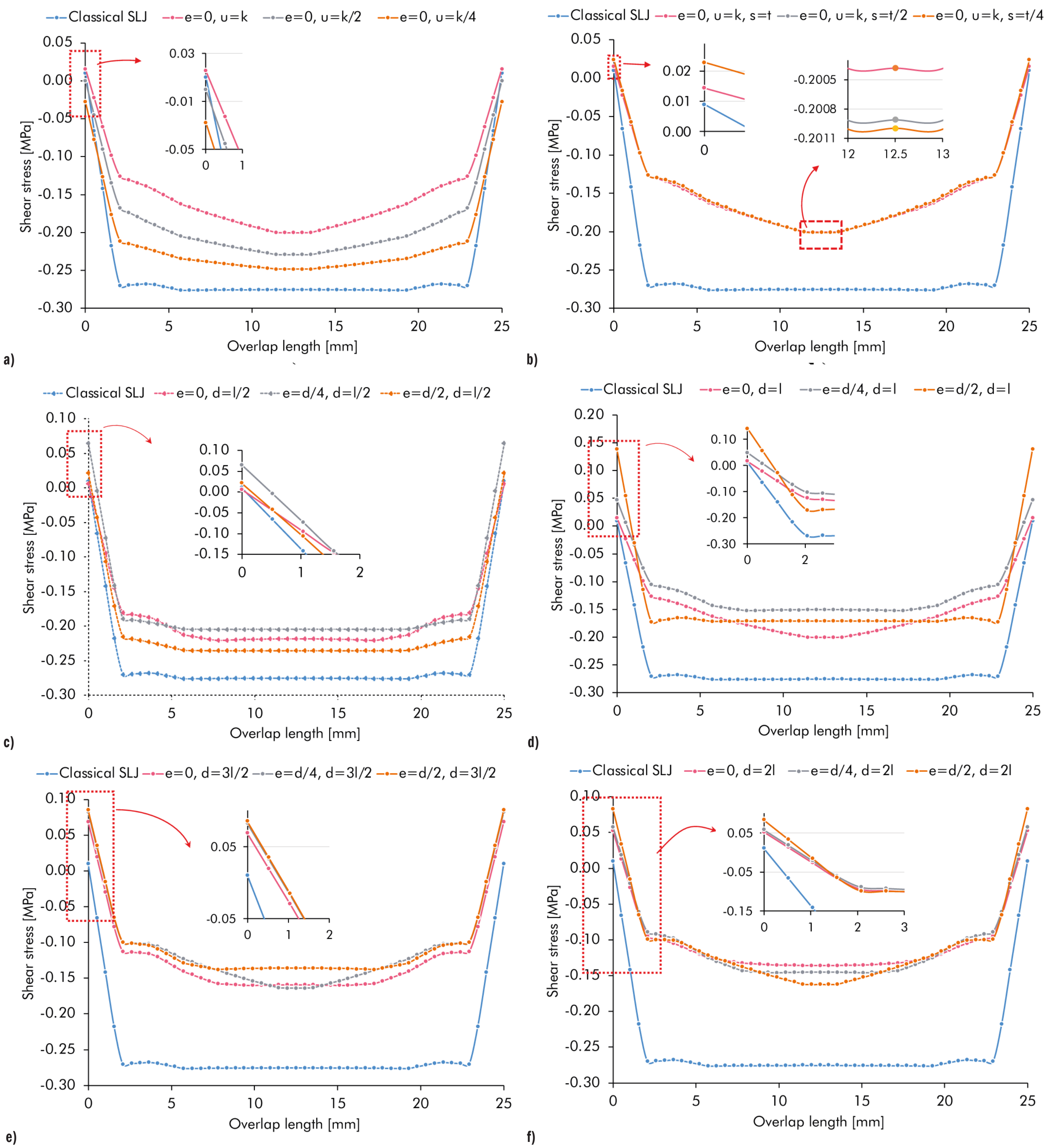

Fig. 9. Shear stress distribution along the length of the overlap zone

$d=3l/2$, and $d=2l$. Moreover, the peel and shear stresses reach their highest values at the midpoint when $d=l/2$. Specifically, when $d=l/2$, the peel stress at the midpoint is 66 % higher compared to $d=$l, and 150 % higher compared to $d=2l$ and $d=2l$. Additionally, the shear stress at the midpoint is 10 % higher for $d=2l$ compared to $d=l$, 37 % higher for $d=3l/2$, and 57 % higher for $d=2l$ (Figs. 8c, d, e, and f).

For $e=d/4$, analysis was performed for various lengths ($d=l/2$, l, $3l/2$, and $2l$). It was found that when the support patch length is equal to the adhesive length ($d=l$), the lowest shear and peel stresses are observed at the edges of the bonded region (Figs. 8c, d, e, and f). In this scenario, the peel stress at the edges is 31 % lower for $d=l/2$, 3 % lower for $d=3l/2$, and 1 % lower for $d=2l$. Additionally, at the midpoint of the bonded region, the peel stress is lowest when $d=2l$. Consequently, for $d=2l$, the peel stress at the midpoint is 60 % lower than for $d=l/2$ and $d=l$, and 50 % lower than for $d=3l/2$. Furthermore, the shear stress at the midpoint is 17 % lower for

$d=l/2$ and $2l$ compared to $d=3l/2$, and 37 % lower for $d=l/2$ and $2l$ compared to $d=3l/2$. The shear stress is lowest at the midpoint when $d=2l$ (Figs. 8c, d, e, and f).

For $e=d/2$, and when the support patch length is 3/2 times the adhesive length ($d=3l/2$), the lowest peel stress is observed at the edges of the bonded region (Figs. 8c, d, e, and f). Specifically, when $d=3l/2$, the peel stress at the edges is 25 % lower for $d=l/2$, 32 % lower for $d=l$, and 2 % lower for $d=2l$. Moreover, at the midpoint of the bonded region, the peel stress is lowest when $d=2l$. Consequently, for $d=2l$, the peel stress at the midpoint is 20 % lower than for $d=l/2$ and $d=l$, and 50 % lower than for $d=3l/2$. For support patch length $d=l/2$, the lowest shear stress is observed at the edges of the bonded region (Figs. 8c, d, e, and f). Specifically, when $d=l/2$, the shear stress at the edges is 85 % lower than for $d=l$, 80 % lower than for $d=3l/2$, and 80 % lower than for $d=2l$. Additionally, at the midpoint, the shear stress is lowest when $d=3l/2$. Consequently, for $d=3l/2$, the shear stress at the midpoint is 58 % lower than for $d=l/2$, 18 % lower than for $d=l$, and 12 % lower than for $d=3l/2$ (Figs. 8c, d, e, and f).

These results demonstrate that the length of the reinforcement patch significantly influences the stress values in the adhesive region and indicate that optimal results can be achieved at specific geometrical parameters.

3.7 The effect of Adhesive Material Properties on Optimal Support Patch Configurations

The optimal configuration of support patches is highly dependent on the mechanical properties of the adhesive material. A more flexible adhesive with lower stiffness and higher elongation capacity would result in a more uniform stress distribution across the bond line. In such a case, support patches with increased length and thickness might be required to counteract the increased deformation and potential stress concentration at the edges. Thicker adhesive layers might be beneficial in reducing peel stresses, thereby allowing a wider range of support patch positions to be effective. On the other hand, a brittle adhesive with higher stiffness and lower fracture toughness would be more sensitive to stress concentrations. In this scenario, it is crucial to design support patches that minimize sharp stress gradients. An optimal design could involve gradual tapering of the support patch edges and the inclusion of fillets to smoothly transfer loads across the adhesive region. Furthermore, smaller patch thicknesses and more centrally positioned patches might be preferred to avoid excessive stress localization at the interface. Recent study provides results about mechanical properties of pressure-sensitive adhesives and the effects of environmental factors, such as thermal shocks, on these properties [34]. It examines the interaction of adhesives with different materials and their resistance to environmental conditions. These insights suggest that while the general trends observed in this study hold, additional experimental and numerical validations are necessary to refine the selection of support patch geometries based on the specific adhesive type employed.

4 DISCUSSIONS

This research presents an in-depth analysis of the effects of support patch geometry on the stress distribution within adhesively bonded SLJs, advancing the understanding of joint behavior and optimization potential. The FE simulations provided a comprehensive evaluation of various patch parameters and their positions, with a particular focus on optimizing the support patch to mitigate stress concentrations, which are critical to the joint's integrity.

The FE results indicate that the dimensions and placement of support patches significantly affect load and stress distribution. For instance, increased support patch thickness (u) correlates with a marked reduction in both peel and shear stresses within the adhesive region, particularly along the joint's edges. Findings underscore the potential of support patches to enhance the mechanical performance of SLJs and, by extension, the reliability of structures that incorporate these joints. It is demonstrated that specific support patch configurations significantly reduce stress concentrations and improve load distribution in adhesive joints. Compared to previous studies, these results show lower stress levels and higher joint durability.

Interestingly, the study also reveals that while the adhesive thickness specific to the support patch significantly reduces peel stress, it has a negligible effect on shear stress. This observation is particularly relevant for structural joint design, where peel stress is a critical factor. It demonstrates the need for a targeted approach for adhesive thickness selection, one that aligns with the specific stress distribution requirements of the joint configuration.

The influence of support patch position (e) also proved to be significant, with optimal patch positioning leading to the lowest stress values at the edges and center of the bonding region. This aspect of the study offers the understanding of how patch positioning can be leveraged to further fine-tune the stress distribution within the joint.

Moreover, the relationship between the support patch length (d) and the bonding length (l) was highlighted as a key factor in determining the effectiveness of the support patch. The results from this study provide a benchmark for selecting appropriate patch lengths, indicating that a patch length equal to the bonding length offers the best performance in terms of stress reduction.

While FEA provides valuable insights into stress distribution, it has limitations in predicting real-world joint performance. Factors such as adhesive defects, environmental effects, and material nonlinearities are not fully captured. Experimental validation through mechanical testing is essential to refine numerical models and enhance their reliability for practical applications. For long-term structural reliability, the impact of environmental factors should be considered. Adhesive materials are known to be sensitive to temperature variations, humidity, and prolonged loading conditions. For instance, at elevated temperatures, some adhesives may experience a decrease in elastic modulus, while at lower temperatures, they may become more brittle, affecting bond strength. Additionally, moisture diffusion into the adhesive interface can weaken adhesion and cause degradation over time. Under sustained loading conditions, creep effects and fatigue behavior become significant concerns. Future studies should focus on experimental validation under temperature- and humidity-controlled environments to assess the durability of optimized patch configurations. Such investigations will enhance the reliability of adhesively bonded joints in long-term engineering applications.

5 CONCLUSIONS

This study investigates the effects of adhesive thickness, position, length, and reinforcement patch thickness on the peel and shear stress distributions in various SLJs. Utilizing the FE model in ANSYS R software, a series of SLJs with different reinforcement patch configurations were simulated. The obtained numerical results underwent detailed analysis to determine the optimized effects of varying adhesive thicknesses, positions, lengths, and thicknesses on the stress distributions of SLJs. The findings obtained are listed below:

- In SSLJs, the peel stress value in the middle part of the bonding region decreases proportionally with an increase in the support patch thickness, while the increase in support patch thickness has not caused a significant change in stress at the edge. Moreover, the increase in support patch thickness results in a greater decrease in peel stress compared to the decrease in shear stress.

- In SLJs, the patch support has a negligible effect on the shear stress at the edges of the bonding region, while it is observed to reduce shear stress values in the middle section of the bonding region.
- Selecting specific ratios for patch adhesive thicknesses in SSLJs significantly reduces peel stress without affecting shear stress values.
- The analysis results indicate that the ratio of support patch length (d) to bonding length (l) has a determining effect on the patch position (e). Specifically, in the case of $d = l/2$, the lowest peel stress values are achieved at $e = 0$, while in the case of $d = 2l$, the highest peel stress values are observed at $e = d/2$.
- It is demonstrated that the optimal bonding performance is achieved when the support patch length is equal to the bonding length.

This study makes a significant contribution to the literature by optimizing support patch geometries in adhesively bonded SLJs. The findings have practical implications for designing more durable and long-lasting adhesive joints in industrial applications.

The FEA conducted in this study has comprehensively revealed the effects of support patches on stress distribution in adhesively bonded single lap joints. However, such numerical studies may be limited unless validated through real-world applications. Future studies should focus on experimentally verifying these numerical results to enhance their reliability. Conducting experiments in accordance with established standards and statistically analyzing the obtained stress data would significantly improve the accuracy and applicability of the findings. Such an approach would not only increase confidence in numerical analyses but also assist engineers in making more reliable design decisions for practical applications. Additionally, the impact of environmental factors, such as temperature variations, humidity, and long-term loading conditions, on the mechanical performance of the optimized patch configurations should be investigated in future research.

References

[1] Alves, D.L., Campilho, R.D.S.G., Moreira, R.D.F., Silva, F.J.G., da Silva, L.F.M. Experimental and Numerical Analysis of Hybrid Adhesively-Bonded Scarf Joints. *Int J Adhes Adhes* 83, 87-95 (2018) **DOI:10.1016/j.ijadhadh.2018.05.011**

[2] Araujo, H.A.M., Machado, J.J.M., Marques, E.S., da Silva, L.F.M. Dynamic Behaviour of Composite Adhesive Joints for the Automotive Industry. *Compos Struct* 171, 549-561 (2017) **DOI:10.1016/j.compstruct.2017.04.049**

[3] Banea, M.D., da Silva, L.F.M., Campilho, R.D.S.G. Principles of Adhesive Bonding. *Joining of Polymer-Metal and Polymer-Polymer Hybrid Structures: Principles and Applications*, p. 3-27 (2018) **DOI:10.1002/9781119429807.ch1**

[4] Gomes, L.A.R., Campilho, R.D.S.G., Valente, J.P.A., Queirós, M.J.R., Madani, K. Impact Loading Analysis of Double-Lap Composite Bonded Joints. *Int J Adhes Adhes* 128, 103547 (2024) **DOI:10.1016/j.ijadhadh.2023.103547**

[5] Fernandez-Canadas, L.M., Ivañez, I., Sanchez-Saez, S., Barbero, E.J. Effect of Adhesive Thickness and Overlap on the Behavior of Composite Single-Lap Joints. *Mech Adv Mater Struct* 28 1111-1120 (2019) **DOI:10.1080/15732479.2019.1573245**

[6] Ozer, H., Oz, O. The Use of the Exponential Drucker-Prager Material Model for Defining the Failure Loads of the Mono and Bi-Adhesive Joints. *Int J Adhes Adhes* 76, 17-29 (2017) **DOI:10.1016/j.ijadhadh.2016.12.006**

[7] Djebbar, N., Boutabout, B., Rachid, H.B., Oudad, W. Effect of Spew Adhesive and Beveling Substrate Geometrical Shape on Stresses in a Bonded Single Lap Joint. *Eng Struct* 256, 114049 (2022) **DOI:10.1016/j.engstruct.2022.114049**

[8] Haddou, Y.M., Salem, M., Amiri, A., Amiri, R., Abid, S. Numerical Analysis and Optimization of Adhesively-Bonded Single Lap Joints by Adherend Notching Using a Full Factorial Design of Experiment. *Int J Adhes Adhes* 126 103482 (2023) **DOI:10.1016/j.ijadhadh.2023.103482**

[9] Demir, K., Bayramoglu, S., Akpinar, S. The Fracture Load Analysis of Different Support Patches in Adhesively Bonded Single-Lap Joints. *Theor Appl Fract Mech* 108 102653 (2020) **DOI:10.1016/j.tafmec.2020.102653**

[10] Amaro, A.M., Neto M.A., Loureiro A., Reis P.N.B. Taper's angle influence on the structural integrity of single-lap bonded joints. *Theor Appl Fract Mech* 96 231-246 (2018) **DOI:10.1016/j.tafmec.2018.06.005**

[11] Çalik, A. Effect of Adherend shape on stress concentration reduction of adhesively bonded single lap joint. *Eng Rev* 36 29-34 (2016)

[12] Afkar, A., Camari, M.N. Finite element analysis of mono- and bi-adhesively bonded functionally graded adherend. *J Fail Anal Prev* 14 253-258 (2014) **DOI:10.1007/s11668-014-9814-5**

[13] Marchione, F. Effect of hollow adherends on stress peak reduction in single-lap adhesive joints: FE and analytical analysis. *J Adhes Sci Technol* 98 656-676 (2021), **DOI:10.1080/00218464.2021.1995368**

[14] Bayramoglu, S., Demir, K., Akpinar, S. Investigation of internal step and metal part reinforcement on joint strength in the adhesively bonded joint: Experimental and numerical analysis. *Theor Appl Fract Mech* 108 102613 (2020) **DOI:10.1016/j.tafmec.2020.102613**

[15] Sancaktar, E., Nirantar, P. Increasing strength of single lap joints of metal adherends by taper minimization. *J Adhes Sci Technol* 17 655-675 (2003), **DOI:10.1163/156856103321340796**

[16] da Silva, L.F.M., Adams, R.D. Techniques to reduce the peel stresses in adhesive joints with composites. *Int J Adhes Adhes* 27 227-235 (2007) **DOI:10.1016/j.ijadhadh.2007.01.001**

[17] Kanani, A.Y., Hou, X., Ye, J. The influence of notching and mixed-adhesives at the bonding area on the strength and stress distribution of dissimilar single-lap joints. *Compos Struct* 241 112136 (2020) **DOI:10.1016/j.compstruct.2020.112136**

[18] Çalik, A., Yildirim, S. An investigation on the effect of parallel slot in Bi-adhesive single lap joints with spew fillet. *J Eng Res* 3 95-110 (2015)

[19] Durmus, M., Akpinar, S. The experimental and numerical analysis of the adhesively bonded three-step-lap joints with different step lengths. *Theor Appl Fract Mech* 105 102427 (2020) **DOI:10.1016/j.tafmec.2019.102427**

[20] Marques, E.A.S., da Silva, L.F.M. Joint strength optimization of adhesively bonded patches. *J Adhes* 84 915-934 (2008) **DOI:10.1080/00218460802427944**

[21] Andruet, R.H., Dillard, D.A., Holzer, S.M. Two- and three-dimensional geometrical nonlinear finite elements for analysis of adhesive joints. *Int J Adhes Adhes* 21 17-34 (2001) **DOI:10.1016/S0143-7496(00)00024-5**

[22] Demiral, M., Mamedov, A. Fatigue performance of a step-lap joint under tensile load: A numerical study. *Polymers* 15 1949 (2023) **DOI:10.3390/polym15081949**

[23] Paygozar, Banea, M.D.S., Sadigh, M.A.S., da Silva, L.F.M. Adhesively bonded aluminium double-strap joints: Effects of patch part on failure load. *J Braz Soc Mech Sci Eng* 42 (2020) **DOI:10.1007/s40430-019-2115-4**

[24] Volkersen, O. Rivet strength distribution in tensile-stressed rivet joints with constant cross-section. *Luftfahrtforschung* 15 41-47 (1938)

[25] Goland, M., Reissner, E. The stresses in cemented joints. *J Appl Mech* 11 A17-A27 (1944), **DOI:10.1115/1.4009336**

[26] ASTM D1002-10 Standard Test Method for Apparent Shear Strength of Single-Lap-Joint Adhesively Bonded Metal Specimens by Tension Loading (Metal-to-Metal) (2019) ASTM Int. **10.1520/D1002-10R19**

[27] Sharma, V.K., Kumar, V., Joshi, R.S. Investigation of rare earth particulate on tribological and mechanical properties of Al-6061 alloy composites for aerospace application. *J Mater Res Technol* 8 3504-3516 (2019) **DOI:10.1016/j.jmrt.2019.06.029**

[28] Khoramishad, H. Effects of mechanical and geometrical properties of adhesive and metal layers on low-velocity impact behavior of metal laminate structures. *J Adhes Sci Technol* 29 592-608 (2015) **DOI:10.1080/01694243.2014.999610**

[29] Bayramoglu, S., Akpinar, S., Calik, A. Numerical analysis of elasto-plastic adhesively single step lap joints using cohesive zone models with experimental verification. *J Mech Sci Technol* 35 641-649 (2021) **DOI:10.1007/s12206-021-0124-0**

[30] Crocombe, A.D., Ashcroft, I.A. Simple Lap Joint Geometry. *Modeling of Adhesively Bonded Joints*. Springer (2008) Berlin Heidelberg 3-23 **DOI:10.1007/978-3-540-79056-3_1**

[31] Ozer, H. Introductory chapter: Structural adhesive bonded joints. *Applied Adhesive Bonding Science and Technology* InTech (2018) **DOI:10.5772/intechopen.74229**

[32] Rodríguez, R.Q., Paiva, W.P., Sollero, P., Albuquerque, E.L., Rodrigues, M.B. Analytical and numerical tools for bonded joint analysis. *Mecánic Comput* 29 7557-7569 (2010)

[33] ANSYS Inc. Academic Research Mechanical Release R2 [Computer software], https://www.ansys.com, accessed on 2023-06-06

[34] Rudawska, A., Wahab, M.A. Mechanical properties of adhesive joints made with pressure-sensitive adhesives. *Stroj Vestn-J Mech E* 67 380-388 (2021) **DOI:10.5545/sv-jme.2021.7253**

Received 2025-01-06, revised 2025-02-21, accepted 2025-03-19,
as Original Scientific Paper.

Data availability *The datasets generated during and/or analyzed during the current study are available from the corresponding author on reasonable request.*

Author contribution *Ahmet Calik: conceptualization, investigation, visualization, writing-original draft, and writing-review and editing.*

Conflicts of interest *The author declares that he has no known competing financial interests or personal relationships that could have appeared to influence the work reported in this paper.*

Optimizacija geometrije podpornih ojačitev pri lepljenih enojnih prekrovnih spojih: Pristop z metodo končnih elementov

Povzetek *V zadnjih letih raziskovalci posvečajo vse več pozornosti uporabi lepljenih spojev v primerjavi s tradicionalnimi metodami, kot so vijačenje ali kovičenje. V tej študiji je uporabljena analiza s pomočjo metode končnih elementov za optimizacijo geometrije in namestitve podpornih ojačitev v lepljenih enojnih prekrovnih spojih, s čimer je možno občutno zmanjšati koncentracije napetosti in izboljšati trdnost spojev. Izvedena je obsežna numerična analiza z metodo končnih elementov, v kateri je preučen vpliv različnih parametrov podpornih ojačitev in njihove lege na trdnost enojnih prekrovnih spojev. Numerični rezultati so validirani s primerjavo z obstoječimi raziskavami iz literature ter analitičnimi rešitvami. Rezultati te raziskave so pokazali, da lahko ustrezna izbira dimenzij in položaja podpornih ojačitev učinkovito zmanjša obremenitve in izboljša porazdelitev napetosti v različnih območjih lepljenega spoja, kar bistveno poveča njegovo trdnost.*

Ključne besede *lepljeni spoji, optimizacija napetosti, geometrija podpornih ojačitev, metoda končnih elementov*